symmetry

MDPI

Article

Impact of Collisional Matter on the Late-Time Dynamics of $f(R,T)$ Gravity

M. Zubair [1,*], Muhammad Zeeshan [1], Syed Sibet Hasan [1] and V. K. Oikonomou [2,3,4]

[1] Department of Mathematics, COMSATS University Islamabad, Lahore Campus, Islamabad 45550, Pakistan; m.zeeshan5885@gmail.com (M.Z.); sibet84@gmail.com (S.S.H.)
[2] Department of Physics, Aristotle University of Thessaloniki, 54124 Thessaloniki, Greece; v.k.oikonomou1979@gmail.com
[3] Laboratory for Theoretical Cosmology, Tomsk State University of Control Systems and Radioelectronics (TUSUR), 634050 Tomsk, Russia
[4] Department of Physics, Tomsk State Pedagogical University, 634061 Tomsk, Russia
* Correspondence: mzubairkk@gmail.com or drmzubair@cuilahore.edu.pk

Received: 23 August 2018; Accepted: 30 September 2018; Published: 5 October 2018

Abstract: We study the cosmic evolution of non-minimally coupled $f(R,T)$ gravity in the presence of matter fluids consisting of collisional self-interacting dark matter and radiation. We study the cosmic evolution in the presence of collisional matter, and we compare the results with those corresponding to non-collisional matter and the Λ-cold-dark-matter (ΛCDM) model. Particularly, for a flat Friedmann–Lemaître–Robertson–Walker Universe, we study two non-minimally coupled $f(R,T)$ gravity models and we focus our study on the late-time dynamical evolution of the model. Our study is focused on the late-time behavior of the effective equation of the state parameter ω_{eff} and of the deceleration parameter q as functions of the redshift for a Universe containing collisional and non-collisional dark matter fluids, and we compare both models with the ΛCDM model. As we demonstrate, the resulting picture is well accommodated to the latest observational data on the basis of physical parameters.

Keywords: $f(R,T)$ gravity; ΛCDM model; dark energy; cosmological parameters

1. Introduction

Recent observations of the accelerated cosmic expansion [1,2] coming from Type Ia supernovae, and the confirmation of the B-mode power spectrum during the early-time inflationary era [3], have utterly changed the perspective of theoretical cosmologists with regard to the evolution of the Universe. The main aim and challenge is to find a unified description of the early and late-time eras, within the same theoretical framework. Modified gravity in general has provided several models that can consistently harbor the early- and late-time evolution of our Universe [4] (see also the reviews [5,6]). With regard to the late-time era, observations support a flat universe formed from pressureless matter with a non-zero cosmological constant Lambda Λ with equation of state (EoS) parameter $\omega = -1$ [7]. Additionally, the latest Planck data [8] favor the Λ-cold-dark-matter (ΛCDM) model for our present epoch, and it seems that the so-called dark energy dominates the evolution of the Universe at the present epoch at a percentage of 69.8% and the luminous matter contributes to the total energy density of our Universe only 4.9% while the remaining 26.8% is controlled by dark matter. The confirmation of the late-time acceleration is further supported by the temperature anisotropies in baryon acoustic oscillations (BAO) [9] and cosmic microwave background (CMB) [10]. As we already mentioned, a consistent way to model the dark energy and the early-time acceleration era is to use the modified gravity theoretical framework [5,6,11–16]. However, alternative approaches can also describe

these acceleration epochs [17–19]. Modified gravity models are generally modifications of the general relativity (GR) picture. In the context of GR, one needs a negative pressure fluid to describe the dark energy era. However, without the use of the modified gravity theoretical framework, one frequently needs phantom fluids to describe an accelerated expansion. There are various modified gravity models in the literature, such as $f(R)$ gravity [20], $f(R,T)$ gravity [21–37], and $f(R,T,R_{\mu\nu}T^{\mu\nu})$ gravity [38–41], where R, T, $R_{\mu\nu}$, and $T^{\mu\nu}$ stand for the Ricci scalar, the trace of the "energy momentum tensor"(EMT), and the Ricci tensor, respectively.

In this paper we use the $f(R,T)$ gravity framework to study the late-time evolution of several cosmological models, in the presence of a collisional matter fluid. We focus our study on the behavior of the EoS parameter ω_{eff} and the deceleration parameter q, as functions of the redshift z. From the latest observational data, we know that the Universe made the deceleration to acceleration transition at a low redshift value $z_t = 0.46 \pm 0.13$ [42]. This transition from a decelerated era to an accelerated one is usually achieved in modified gravity models (e.g., [4,43–47]), and the aim in this paper is to investigate if a viable late-time phenomenology can be achieved for $f(R,T)$ models of gravity in the presence of collisional matter. Similar studies in the context of $f(R)$ gravity have been performed in [48,49], so in this paper we extend these in the context of $f(R,T)$ gravity. Also, in Ref. [50–52], the dark energy dominance and the deceleration to acceleration transition was studied in the presence of cold dark matter for $f(T)$ models. In addition, in Ref. [53] the late-time behavior of $f(R,T)$ gravity models was compared to the ΛCDM model, with good agreement (see also Refs. [28,54–61] for additional studies in the field). In this work, the collisional matter fluid mainly refers to the presence of a logarithmic term in the EoS parameter of the dark matter fluid. The $f(R,T)$ gravity part will drive the late-time acceleration, so we mainly aim to see whether the presence of collisional matter alters the late-time behavior of the $f(R,T)$ model, and to which extent the model can be comparable to the ΛCDM.

This paper is organized as follows: In Section 2, we briefly review the $f(R,T)$ theoretical framework by presenting the general formalism of the model. In Section 3, we incorporate a collisional matter component in the EoS of dark matter and we express the field equations as functions of the redshift, and we study the behavior of the EoS parameter and of the deceleration parameter as functions of the redshift parameter z, for two characteristic models of $f(R,T)$ gravity. Finally, the conclusions follow at the end of the paper.

2. $f(R,T)$ Gravity: Basic Formalism

In this section, we discuss the basic formulation of $f(R,T)$ gravity and its corresponding field equations for a Friedmann–Lemaître–Robertson–Walker (FLRW) spacetime in the presence of ordinary matter. The line element of the FLRW metric is

$$ds^2 = dt^2 - a^2(t)d\mathbf{x}^2, \tag{1}$$

where $a(t)$ is the scale factor and the corresponding Ricci scalar is

$$R = -6(2H^2 + \dot{H}),$$

where H is the Hubble parameter and "dot" denotes differentiation with respect to cosmic time t. The action of $f(R,T)$ gravity is [21]

$$S = \frac{1}{\kappa^2}\int f(R,T)\sqrt{-g}d^4x + \int \mathcal{L}_m\sqrt{-g}d^4x, \tag{2}$$

where $f(R,T)$ is an arbitrary function of Ricci scalar R and of the trace of the EMT $T = g^{\mu\nu}T_{\mu\nu}$. In addition, $\kappa^2 = 1/M_p^2$, where M_p is the Planck mass scale. Here $\mathcal{L}_m$ represents the Lagrangian

density of ordinary matter. By varying the above action with respect to the metric tensor, we have the following set of equations:

$$8\pi T_{\mu\nu} - f_T(R,T)T_{\mu\nu} - f_T(R,T)\Theta_{\mu\nu} = f_R(R,T)R_{\mu\nu} - \tfrac{1}{2}f(R,T)g_{\mu\nu} + (g_{\mu\nu}\Box - \nabla_\mu\nabla_\nu)f_R(R,T). \quad (3)$$

By contracting the above equation, we acquire a relation between Ricci scalar R and the trace T of the EMT:

$$8\pi T - f_T(R,T)T - f_T(R,T)\Theta = f_R(R,T)R + 3\Box f_R(R,T) - 2f(R,T). \quad (4)$$

These two equations contain the covariant derivative and the d'Alembert operator denoted by ∇ and $\Box$, respectively. Furthermore, $f_R(R,T)$ and $f_T(R,T)$ correspond to the functional derivatives of $f(R,T)$ with respect to R and T, respectively. Additionally, the term $\Theta_{\mu\nu}$ is defined as follows:

$$\Theta_{\mu\nu} = \frac{g^{\alpha\beta}\delta T_{\mu\nu}}{\delta g^{\mu\nu}} = -2T_{\mu\nu} + g_{\mu\nu}L_m - 2g^{\alpha\beta}\frac{\partial^2 L_m}{\partial g^{\mu\nu}\partial g^{\alpha\beta}}.$$

The EMT for an isotropic perfect fluid is given by,

$$T_{\mu\nu} = (\rho_m + P_m)u_\mu u_\nu - P_m g_{\mu\nu},$$

where u_μ is the four-velocity of the fluid. Here, we choose $\mathcal{L}_m = -P_m$, which leads to following expression for $\Theta_{\mu\nu}$:

$$\Theta_{\mu\nu} = -2T_{\mu\nu} - P_m g_{\mu\nu}. \quad (5)$$

With the help of Equation (5), the field Equation (3) can be written in the following form:

$$R_{\mu\nu} - \frac{1}{2}Rg_{\mu\nu} = k_{eff}^2 T_{\mu\nu}^{eff}, \quad (6)$$

where $k_{eff}^2 = \frac{k^2+f_T}{f_R}$ is the effective gravitational constant, and

$$T_{\mu\nu}^{eff} = T_{\mu\nu} + \frac{1}{k^2+f_T}\left[\frac{1}{2}g_{\mu\nu}(f - Rf_R) + f_T P_m g_{\mu\nu} - (g_{\mu\nu} - \nabla_\mu\nabla_\nu)f_R\right] \quad (7)$$

is the effective EMT.

Applying the covariant divergence to the field Equation (3), one can find [62]:

$$\nabla^\alpha T_{\alpha\beta} = \frac{f_T}{\kappa^2 - f_T}\left[(T_{\alpha\beta} + \Theta_{\alpha\beta})\nabla^\alpha \ln f_T + \nabla^\alpha\Theta_{\alpha\beta} - \frac{1}{2}g_{\alpha\beta}\nabla^\alpha T\right]. \quad (8)$$

It is important to see that any modified theory which involves non-minimal coupling between geometry and matter does not obey the ideal continuity equation. $f(R,T)$ also involves this type of non-minimal coupling, so it also deviates from standard behavior of continuity equations. Here, non-minimal coupling between matter and geometry induces extra force acting on massive particles, whose equation of motion is given by [62]:

$$\frac{d^2x^\lambda}{ds^2} + \Gamma^\lambda_{\mu\nu}u^\mu u^\nu = f^\lambda,$$

where

$$f^\lambda = \frac{8\pi\nabla_\nu p - \frac{1}{2}f_T(R,T)\nabla_\nu T}{(\rho+p)(8\pi + f_T(R,T))}(g^{\mu\nu} - u^\mu u^\nu).$$

The matter energy density ρ_m satisfies the following continuity equation:

$$\dot{\rho_m} + 3H(\rho_m + P_m) = \frac{-1}{\kappa^2 + f_T}\left[(\rho_m + P_m)\dot{T}f_{TT} + \dot{P_m}f_T + \frac{1}{2}\dot{T}f_T\right]. \tag{9}$$

To obtain the standard continuity equation, we need to have an additional constraint by setting the right side of the above equation equal to zero. For the EoS $P_m = \omega\rho_m$, Equation (9) becomes:

$$\dot{\rho_m} + 3H\rho_m(1+\omega) = 0, \tag{10}$$

with constraint

$$(1+\omega)Tf_{TT} + \frac{1}{2}(1-\omega)f_T = 0. \tag{11}$$

In [61], authors reconstructed some well-known models of $f(R,T)$ theory of gravity corresponding to cosmological evolution including ΛCDM, phantom or non-phantom eras and possible phase transition from accelerating to decelerating by keeping the energy momentum tensor covariantly conserved. They utilized the additional constraint (11) in the comprehensive reconstruction scheme. We opted to follow two generic models of the form

- $f(R,T) = \alpha_1 R^{\gamma_1} T^{\gamma_2} + \alpha_2 T$,
- $f(R,T) = \beta_1 R^{\mu} + \beta_2 R^{\nu} + \frac{2k^2}{-1+3\omega}T + \beta_3 T^{\frac{1}{2} - \frac{\sqrt{-1+\omega(3+\omega-3\omega^2)}}{(1+\omega)\sqrt{-2+6\omega}}} + \beta_4 T^{\frac{1}{2} + \frac{\sqrt{-1+\omega(3+\omega-3\omega^2)}}{(1+\omega)\sqrt{-2+6\omega}}}$.

The significant aspects of this choice: these models represent the non-minimal coupling of curvature R and matter components T (as compared to previous studies [53]), and are reconstructed for the conserved energy momentum tensor. In the next section we will consider effective fluid to develop a generic equation involving the role of collisional fluid.

3. Collisional Matter Model within $f(R,T)$ Theory and Late-Time Dynamics

The analytical results of high-energy particle detectors such as ATIC, PAMELA, and WMAP indicate that the production of the electron–positron in the Universe is larger compared to that observed by cosmic ray collisions and by supernova SNIa explosions [63]. This issue helps us to find the total destruction rate of weakly interacting matter particles, and this process is collisional [64]. The effects of collisional matter in the Universe's evolution were considered in Ref. [65] in the context of Einstein–Hilbert gravity, and the same problem was considered in Refs. [48,49] in the context of $f(R)$ gravity. As was shown in Refs. [48,49], a transition from deceleration to acceleration can be achieved, and in this paper we shall investigate whether this transition can occur in the context of $f(R,T)$ gravity, and whether the resulting picture can be comparable with the ΛCDM model. Mostly, self-interacting collisional matter models are quantified in terms of a perfect fluid in which total mass-energy density denoted by ϵ_m depends on two terms, as follows:

$$\epsilon_m = \rho_m + \rho_m\Pi, \tag{12}$$

where Π stands for

$$\Pi = \Pi_0 + \omega ln(\frac{\rho_m}{\rho_{m_0}}), \tag{13}$$

where ρ_{m_0} and Π_0 are present day values. In this case, the pressure of the collisional matter fluid is

$$P_m = \omega\rho_m, \tag{14}$$

where the EoS parameter of the collisional dark matter fluid is represented by ω and $0 < \omega < 1$. Using Equations (12) and (13), we obtain the following relation of the total energy density of the Universe:

$$\epsilon_m = \rho_m(1 + \Pi_0 + \omega ln(\frac{\rho_m}{\rho_{m_0}})). \tag{15}$$

The energy momentum conservation is quantified by the following equation:

$$\nabla^\nu T_{\mu\nu} = 0\,, \tag{16}$$

and the EMT becomes as follows:

$$T_{\mu\nu} = (\epsilon_m + P_m)u_\mu u_\nu - P_m g_{\mu\nu}, \tag{17}$$

where $u_\mu = \frac{dx_\mu}{ds}$ is the four-velocity and satisfies the equation $u_\mu u^\mu = 1$. Using the FLRW line element given in (1), the energy–momentum conservation equation has the following form:

$$\dot{\epsilon_m} + 3\frac{\dot{a}}{a}(\epsilon_m + P_m) = 0\,. \tag{18}$$

Combining Equations (14) and (15), we obtain the following result:

$$\rho_m = \rho_{m_0}\left(\frac{a_0}{a}\right)^3, \tag{19}$$

where a_0 is the current value of the scale factor. Here we can see that collisional matter can be described by Equations (15) and (19). In addition, Π_0 has the value

$$\Pi_0 = \left(\frac{1}{\Omega_M} - 1\right), \tag{20}$$

and its numerical value is $\Pi_0 = 2.14169$. There is an important case that needs to be discussed, related to the fact that our Universe is filled with both matter and radiation. To this end, we assume that apart from collisional matter, the Universe is also filled with radiation, so the total energy density of the matter fluids is:

$$\rho_{matt} = \epsilon_m + \rho_{r0}a^{-4}, \tag{21}$$

where ρ_{r0} represents the present energy density for the radiation fluid. The total pressure in this case is given by

$$P_{matt} = p_m + p_r, \tag{22}$$

where p_m is the pressure for collisional matter and p_r is the pressure from radiation. By using Equations (15) and (19), we can rewrite Equation (21) in the following form:

$$\rho_{matt} = \rho_{m0}a^{-3}(1 + \Pi_0 - 3\omega ln(a)) + \rho_{r0}a^{-4}. \tag{23}$$

We can also rewrite Equation (23) as follows:

$$\rho_{matt} = \rho_{m0}(g(a) + \chi a^{-4}), \tag{24}$$

where χ is defined as $\chi = \frac{\rho_{r0}}{\rho_{m0}}$, its numerical value is $\chi = 3.1 \times 10^{-4}$. In addition, $g(a)$ is defined as follows:

$$g(a) = a^{-3}(1 + \Pi_0 - 3\omega ln(a))\,. \tag{25}$$

In the above cases, if we set $\omega = 0$, $\Pi_0 = 0$, we recover the standard cold dark matter case, and in addition if we take $\chi = 0$, the radiation fluid makes no contribution to the energy density of our Universe.

Now, let us proceed in the calculation of the total EoS parameter of the $f(R,T)$ model and of the deceleration parameter $q(z)$ as functions of the redshift parameter defined in terms of the scale factor as follows $1 + z = 1/a$. The field equations are rewritten as follows:

$$3H^2 = \frac{1+f_T}{f_R}\epsilon_m + \frac{1}{f_R}[\frac{1}{2}(f - Rf_R) - 3\dot{R}Hf_{RR} + P_m f_T], \tag{26}$$

$$-2\dot{H} - 3H^2 = \frac{1+f_T}{f_R}P_m + \frac{1}{f_R}[2\dot{R}Hf_{RR} + \ddot{R}f_{RR} + \dot{R}^2 f_{RRR} - \frac{1}{2}(f - Rf_R) - P_m f_T]\,, \tag{27}$$

where $H = \frac{\dot{a}}{a}$ is the Hubble parameter. We rewrite the right hand side of Equations (26) and (27) in terms of effective energy density ρ_{eff} and of the effective pressure P_{eff} as follows:

$$3H^2 = {k^2}_{eff}\rho_{eff}, \tag{28}$$

$$-2\dot{H} - 3H^2 = {k^2}_{eff}P_{eff}. \tag{29}$$

Here ${k^2}_{eff} = \frac{1+f_T}{f_R}$ and ρ_{eff}, P_{eff} have the following form:

$$\rho_{eff} = \epsilon_m + \frac{1}{1+f_T}[\frac{1}{2}(f - Rf_R) - 3\dot{R}Hf_{RR} + P_m f_T], \tag{30}$$

$$P_{eff} = P_m + \frac{1}{1+f_T}[2\dot{R}Hf_{RR} + \ddot{R}f_{RR} + \dot{R}^2 f_{RRR} - \frac{1}{2}(f - Rf_R) - P_m f_T]. \tag{31}$$

The energy density of dark energy is equal to $\rho_{DE} = \rho_{eff} - \epsilon_m$, and the corresponding pressure is $P_{DE} = P_{eff} - P_m$. The energy momentum conservation is

$$\frac{d(k^2_{eff}\rho_{eff})}{dt} + 3Hk^2_{eff}(\rho_{eff} + P_{eff}) = 0. \tag{32}$$

Using Equations (28) and (29), the above equation takes the form

$$18\frac{f_{RR}}{f_R}H(\ddot{H} + 4H\dot{H}) + 3(\dot{H} + H^2) + \frac{1+f_T}{f_R}\epsilon_m + P_m\frac{f_T}{f_R} + \frac{f}{2f_R} = 0. \tag{33}$$

Using the redshift parameter $z = \frac{1}{a} - 1$, the above equation can be written as follows:

$$\frac{d^2H}{dz^2} = \frac{3}{1+z}\frac{dH}{dz} - \frac{1}{H}(\frac{dH}{dz})^2 - \frac{3f_R(H^2 - (1+z)H\frac{dH}{dz}) + \frac{f}{2} + P_m f_T + (1+f_T)\epsilon_m}{18H^3 f_{RR}(1+z)^2}. \tag{34}$$

In the rest of this section, we will study the late-time evolution of the Universe filled with collisional matter and radiation, for two characteristic models of $f(R,T)$ gravity. To this end we will numerically solve the differential Equation (34) for $H(z)$, and we shall calculate the corresponding total equation of state parameter and deceleration parameter as functions of the redshift z. With regards to the deceleration parameter as a function of the redshift, we shall use the following formula:

$$q(z) = \frac{1+z}{H(z)}\frac{dH(z)}{dz} - 1\,. \tag{35}$$

Accordingly, we shall compare the collisional matter $f(R,T)$ gravity with the non-collisional matter late-time evolution. We shall consider two different values for the EoS parameter of the collisional matter, namely $\omega = 0.5$ and $\omega = 0.8$. Moreover, the observational value for present Hubble

parameter is taken $H_0 = 68.3$, and finally the fractional energy density of dark matter at present day is $\Omega_{m0} = 0.24$.

3.1. $f(R,T)$ Model I

Let us first consider a pure non-minimally coupled $f(R,T)$ model gravity of the form $f(R,T) = \alpha_1 R^{\gamma_1} T^{\gamma_2} + \alpha_2 T$. In Ref. [61], the authors reconstructed this model and investigated the instability of the model against density matter perturbations and the Dolgov–Kawasaki instability criterion.

In order for this model to be viable, the following condition must hold true:

$$f_{RR} = \alpha_1 \gamma_1 (\gamma_1 - 1) R^{\gamma_1 - 2} T^{\gamma_2} \geq 0\,, \tag{36}$$

so we need to have $\gamma_1 > 1$ and $\alpha_1 > 0$. For the numerical analysis, we choose the free parameters values as follows: $\alpha_1 = 20, \alpha_2 = 15$, $H_0 = 68.3$, and $\Omega_m = 0.3183$. We employ the numerical approach to find $H(z)$ by solving Equation (34). We investigate the behavior of the total EoS parameter, ω_{eff}, and of ω_{DE} for non-collisional matter and collisional matter. We present two different cases depending on the exponents of R and T in the above model. For the first model, we set $\gamma_1 = 10$ and $\gamma_2 = -0.7$, so that $f(R,T)$ takes the form

- $\alpha_1 R^{10} T^{-4/5} + \alpha_2 T\,.$

In the left plot of Figure 1 we present the evolution of the deceleration parameter for four different cases in terms of the redshift z. The blue curve represents the standard ΛCDM model, the green curve is for non-collisional matter, the black curve represents collisional matter, and the red curve represents collisional matter in the presence of radiation. We can clearly see from Figure 1 that the behavior of the green curve and red curve correspond to the ΛCDM, but the black curve is lower than the blue curve and changes its behavior. We can also observe the deceleration to acceleration transition point in the left plot of Figure 1 for the aforementioned cases. In the case of non-collisional matter, collisional matter, the transition from deceleration to acceleration is almost equal to the one corresponding to the ΛCDM model, and it is equal to $z_t = 1.9$. For the collisional matter case, the transition point is at $z_t = 7.6$ and this is larger than observations. In the right plot of Figure 1, we present the evolution of the total EoS parameter for non-collisional matter, collisional matter, and for collisional matter plus radiation. In all cases, the total EoS parameter ω_{eff} approaches the phantom divide line value $\omega_{eff} = -1$ but it does not cross it, for all the models, at least up to the present value of the redshift (which is ($z = 0$). Also in Figure 2, we present the behavior of the Hubble rate as a function of the redshift (left plot) and of the dark energy density as a function of the redshift (right plot). As can be seen in both figures, the collisional matter phenomenology is qualitatively viable.

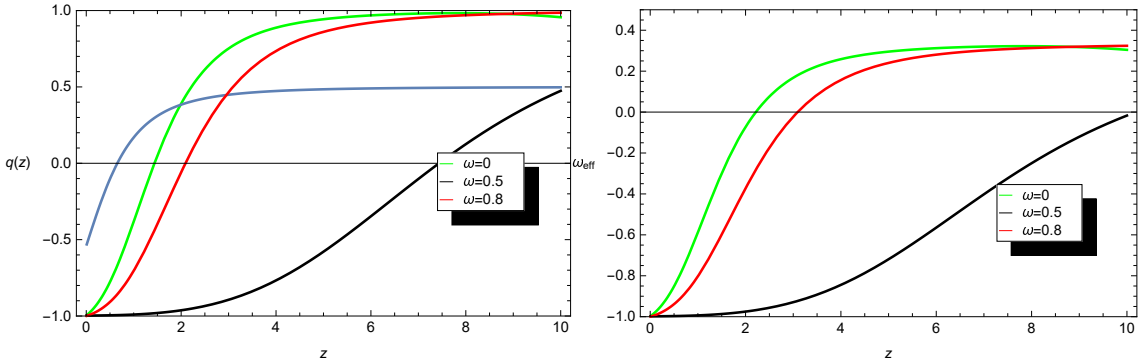

Figure 1. The evolution of deceleration parameter versus redshift z (**left**) plot and the evolution of total effective equation of state (EoS) parameter versus the redshift z (**right**) plot. The free parameter values were chosen to be $\alpha_1 = 20, \alpha_2 = 15, \gamma_1 = 10$, $\gamma_2 = -0.7$, and $\Omega_m = 0.3183$.

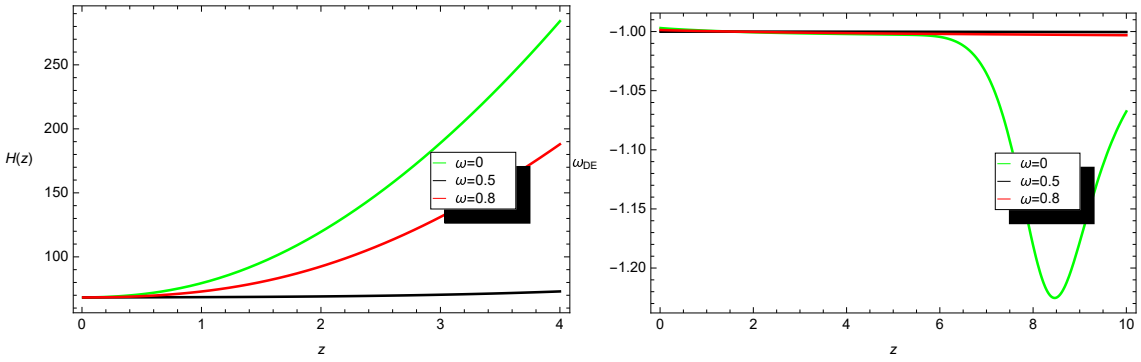

Figure 2. The evolution of $H(z)$ versus redshift z (**left**) and the evolution of the dark energy EoS parameter versus the redshift z (**right**). The free parameter values are $\alpha_1 = 20, \alpha_2 = 15, \gamma_1 = 10$, $\gamma_2 = -0.7$, and $\Omega_m = 0.3183$.

3.2. $f(R,T)$ *Model II*

Let us now consider the following $f(R,T)$ model:

$$f(R,T) = \beta_1 R^{\mu} + \beta_2 R^{\nu} + \frac{2k^2}{-1+3\omega} T + \beta_3 T^{\frac{1}{2} - \frac{\sqrt{-1+\omega(3+\omega-3\omega^2)}}{(1+\omega)\sqrt{-2+6\omega}}} + \beta_4 T^{\frac{1}{2} + \frac{\sqrt{-1+\omega(3+\omega-3\omega^2)}}{(1+\omega)\sqrt{-2+6\omega}}}. \quad (37)$$

This model is of the form $f(R,T) = f(R) + f(T)$, and the second derivative of this model with respect to the Ricci scalar is

$$f_{RR} = \beta_1 \mu(\mu-1) R^{\mu-2} + \beta_2 \nu(\nu-1) R^{\nu-2} \geq 0. \quad (38)$$

The validity of this model crucially depends on second-derivative f_{RR} which should be greater than zero, which means $\mu > 1, \nu > 1, \beta_1 > 0$, and $\beta_2 > 0$. We chose the free variables values as follows: $(\beta_1, \beta_2, \beta_3, \beta_4, \mu, \nu) = (5, 10, 15, 20, 25, 30)$, and $\Omega_m = 0.3183$. We numerically study this $f(R,T)$ model by solving the differential Equation (34). In Figure 3 we present the results of our study, and specifically in the left plot we present the deceleration parameter as a function of the redshift and in the right plot we present the total EoS parameter as a function of the redshift. The conventions for the colored curves are the same as in the previous model—that is, the blue curve represents the results for the ΛCDM model, the green curve represents the non-collisional matter, and the black curve stands for the collisional matter. Finally, the red curve represents the collisional matter when radiation is also considered. As can be seen, this model is in better agreement with the ΛCDM model, and also the transition point from deceleration to acceleration for all cases containing collisional matter are closer to the ΛCDM model. Moreover, in Figure 4 we plot the Hubble rate as a function of the redshift (left plot) and the EoS parameter for the dark energy sector. As can be seen, the results are in good qualitative agreement with the late-time phenomenological picture. In addition, the value of the Hubble rate today was calculated to be 68.4, which is a very good approximation of the actual present day value $H_0 = 68.3$.

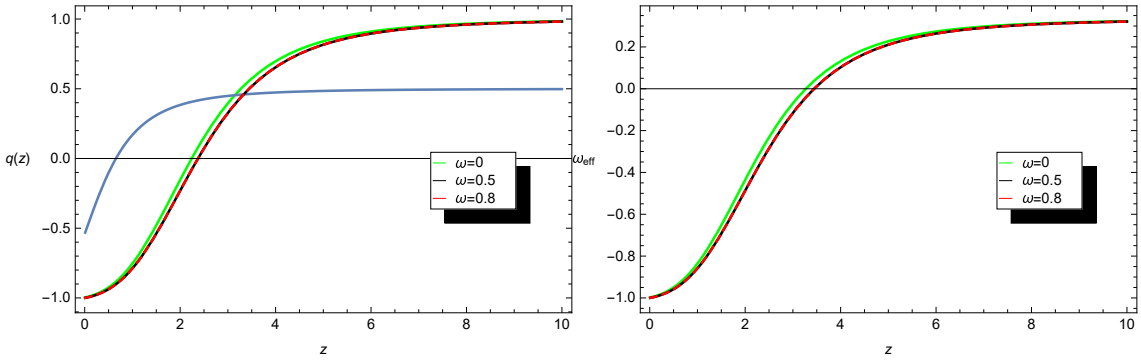

Figure 3. The evolution of deceleration parameter versus redshift z (**left**) and the evolution of the total EoS parameter versus redshift z (**right**). The free parameter values were chosen to be $\beta_1 = 5, \beta_2 = 10, \beta_3 = 15, \beta_4 = 20, \mu = 25, \nu = 30$, and $\Omega = 0.3183$.

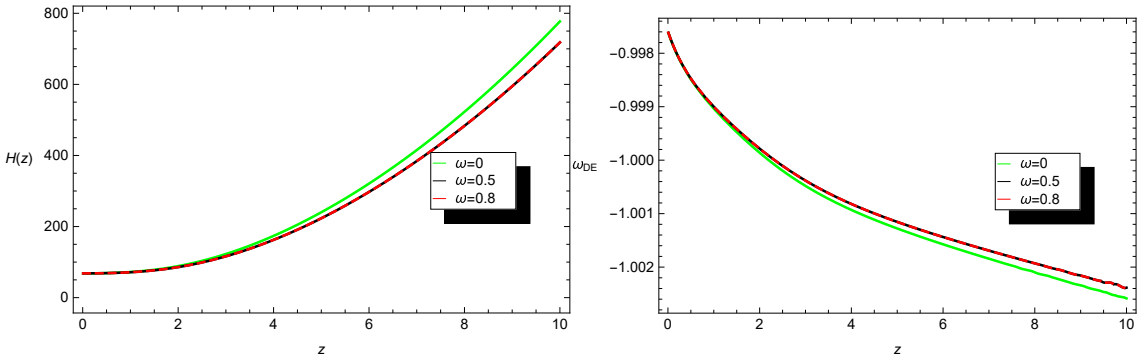

Figure 4. The evolution of $H(z)$ versus redshift z (**left**) and the evolution of the dark energy EoS parameter versus the redshift z (**right**). The free parameter values were chosen to be $\beta_1 = 5$, $\beta_2 = 10$, $\beta_3 = 15$, $\beta_4 = 20$, $\mu = 25$, $\nu = 30$, and $\Omega = 0.3183$.

3.3. Another Perspective of the Late-Time Cosmological Evolution of Dark Energy with Collisional Matter Fluid

In this section we specialize the dark energy study by using appropriately chosen variables. In this way we also discuss the issue of dark energy oscillations, which haunts several modified gravity models (see for example [5] for a review of this issue). The field Equation (26) for the flat FLRW metric takes the following form:

$$3H^2 f_R = (1 + f_T)\rho_{matt} + \frac{1}{2}(f - Rf_R) - 3\dot{R}Hf_{RR} + P_{matt}f_T. \tag{39}$$

Equation (39) can also be written as follows:

$$\frac{1}{\bar{m}^2}\frac{dR}{dlna} = \frac{1}{H^2 f_{RR}}\left[\frac{f_T}{3\bar{m}^2}(\rho_{matt} + P_{matt}) + \frac{1}{3\bar{m}^2}\rho_{matt} - \frac{H^2}{\bar{m}^2} + \frac{1}{6\bar{m}^2}(f - R) - (1 - f_R)\left(\frac{H}{\bar{m}^2}\frac{dH}{dlna} + \frac{H^2}{\bar{m}^2}\right)\right]. \tag{40}$$

We introduce the following variables [49] in order to make the study of the late-time cosmological evolution of $f(R, T)$ theory more focused:

$$y_H \equiv \frac{\rho_{DE}}{\rho_{m_0}} = \frac{H^2}{\bar{m}^2} - g(a) - \chi a^{-4}, \tag{41}$$

$$y_R \equiv \frac{R}{\bar{m}^2} - \frac{dg(a)}{dlna}. \tag{42}$$

Here ρ_{DE} denotes the energy density of the dark energy, $\bar{m}^2$ is the mass scale given by [48] $\bar{m}^2 = \frac{k^2\rho_{m_0}}{3}$. Using Equations (40)–(42), we obtain the following set of differential equations:

$$\frac{dy_H}{dlna} = -\frac{1}{3}y_R - 4y_H - \frac{4}{3}\frac{dg(a)}{dlna} - 4g(a), \tag{43}$$

$$\begin{aligned}\frac{dy_R}{dlna} = &-\frac{d^2g(a)}{dlna^2} + \frac{1}{\bar{m}^2(y_H+g(a)+\chi a^{-4})f_{RR}}[\frac{f_T}{3\bar{m}^2}(\rho_{matt}+P_{matt}) - y_H + \frac{1}{6\bar{m}^2}(f-R)\\ &-(1-f_R)(\tfrac{1}{2}\frac{dy_H}{dlna} + \tfrac{1}{2}\frac{dg(a)}{dlna} + y_H + g(a) - \chi a^{-4})].\end{aligned} \tag{44}$$

The curvature scalar can also be written in the form

$$R = -3\bar{m}^2(4y_H + 4g(a) + \frac{dy_H}{dlna} + \frac{dg(a)}{dlna}). \tag{45}$$

Now making use of Equations (43) and (44), we obtain

$$\begin{aligned}&-3\frac{d^2y_H}{dlna^2} - 12\frac{dy_H}{dlna} - 3\frac{d^2g(a)}{dlna^2} - 12\frac{dg(a)}{dlna} = \frac{1}{\bar{m}^2(y_H+g(a)+\chi a^{-4})f_{RR}}[\frac{f_T}{3\bar{m}^2}(\rho_{matt}+P_{matt}) - y_H\\ &+\frac{1}{6\bar{m}^2}(f-R) - (1-f_R)(\tfrac{1}{2}\frac{dy_H}{dlna} + \tfrac{1}{2}\frac{dg(a)}{dlna} + y_H + g(a) - \chi a^{-4})] = 0.\end{aligned} \tag{46}$$

Rearranging the terms, we finally obtain the following differential equation:

$$\begin{aligned}&\frac{d^2y_H}{dlna^2} + (4 - \frac{1-f_R}{6\bar{m}^2(y_H+g(a)+\chi a^{-4})f_{RR}})\frac{dy_H}{dlna} + \frac{f_R-2}{3\bar{m}^2(y_H+g(a)+\chi a^{-4})f_{RR}}y_H + \frac{d^2g(a)}{dlna^2}\\ &+(4 + \frac{f_R-1}{6\bar{m}^2(y_H+g(a)+\chi a^{-4})f_{RR}})\frac{dg(a)}{dlna} + \frac{f_R-1}{3\bar{m}^2(y_H+g(a)+\chi a^{-4})f_{RR}}g(a) + \frac{1-f_R}{3\bar{m}^2(y_H+g(a)+\chi a^{-4})f_{RR}}\\ &\chi a^{-4} + \frac{f-R}{18\bar{m}^4(y_H+g(a)+\chi a^{-4})f_{RR}} - \frac{g(a)+\omega a^{-3}+(1+\omega)\chi a^{-4}}{3\bar{m}^2(y_H+g(a)+\chi a^{-4})f_{RR}}[\frac{f_T}{3\bar{m}^2}(\rho_{matt}+P_{matt})] = 0.\end{aligned} \tag{47}$$

By making use of redshift $z = \frac{1}{a} - 1$ in conjunction with the relations

$$\frac{d}{dlna} = -(1+z)\frac{d}{dz}, \tag{48}$$

$$\frac{d^2}{dlna^2} = (1+z)^2\frac{d^2}{dz^2} + (1+z)\frac{d}{dz}, \tag{49}$$

we can rewrite the differential Equation (47) as follows:

$$\begin{aligned}&(1+z)^2\frac{d^2y_H}{dz^2} + (1+z)\frac{dy_H}{dz} - (1+z)(4 - \frac{1-f_R}{6\bar{m}^2(y_H+g(z)+\chi(1+z)^4)f_{RR}})\frac{dy_H}{dz} + \frac{f_R-2}{(y_H+g(z)+\chi(1+z)^4)}\\ &\frac{y_H}{3\bar{m}^2f_{RR}} + (1+z)^2\frac{d^2g(z)}{dz^2} + (1+z)\frac{dg(z)}{dz} - (1+z)(4 + \frac{f_R-1}{6\bar{m}^2(y_H+g(z)+\chi(1+z)^4)f_{RR}})\frac{dg(z)}{dz}\\ &+\frac{f_R-1}{3\bar{m}^2(y_H+g(z)+\chi(1+z)^4)f_{RR}}g(z) + \frac{1-f_R}{3\bar{m}^2(y_H+g(z)+\chi(1+z)^4)f_{RR}}\chi(1+z)^4 + \frac{f-R}{(y_H+g(z)+\chi(1+z)^4)}\\ &\frac{1}{18\bar{m}^4f_{RR}} - \frac{g(z)+\omega(1+z)^3+(1+\omega)\chi(1+z)^4}{3\bar{m}^2(y_H+g(z)+\chi(1+z)^4)f_{RR}}[\frac{f_T}{3\bar{m}^2}(\rho_{matt}+P_{matt})] = 0.\end{aligned} \tag{50}$$

The focus in this section is on numerically solving the differential Equation (50) and thus finding the exact behavior of the function $y_H \equiv \frac{\rho_{DE}}{\rho_{m_0}}$. This will make apparent the existence or not of dark energy oscillations in any of the models. We also compare the behavior of the collisional matter $f(R,T)$ gravity in the presence and absence of radiation, with the non-collisional matter case. Consider first the model I which we studied previously, and after solving the differential Equation (50), we present the results of our study in Figure 5. Particularly, in the left plot of Figure 5, we plot the behavior of the function $y_H(z)$ as a function of z, and in the left plot we plot the dark energy EoS parameter $\omega_{DE}(z) = \frac{P_{DE}}{\rho_{DE}}$, which in terms of $y_H(z)$ is equal to

$$\omega_{DE}(z) = -1 + \frac{1}{3}(1+z)\frac{1}{y_H}\frac{dy_H}{dz}. \tag{51}$$

Also in all the plots we assume the following values for the free parameters of the models: $\gamma_1 = 10$, $\gamma_2 = -0.7$, $\alpha_1 = 20, \alpha_2 = 15$, $H_0 = 68.3$, and $\Omega_m = 0.3183$. As in the previous cases, the red curves in the plots of Figure 5 correspond to collisional matter with radiation, the green curve corresponds to collisional matter without radiation, and the black corresponds to non-collisional matter. As can be seen, the presence of collisional matter on the cosmological model slightly changes the quantitative picture of the model, but the qualitative behavior is not altered. Thus, by using the formalism we presented in this section, we demonstrated that the presence of collisional matter provides us with qualitatively viable phenomenology.

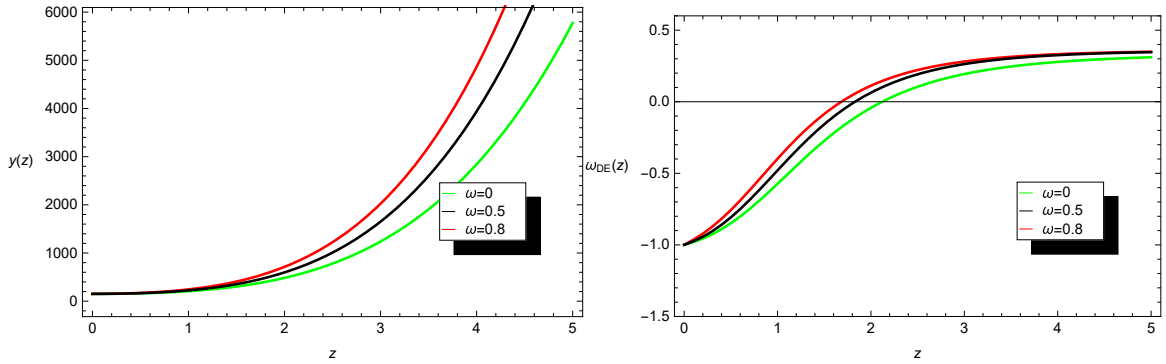

Figure 5. The evolution of $y_H(z)$ as a function of the redshift (**left**), and the evolution of the dark energy EoS parameter as a function of the redshift (**right**). The free parameter values were chosen to be, $\alpha_1 = 20, \alpha_2 = 15, \gamma_1 = 10$, $\gamma_2 = -0.7$, and $\Omega_m = 0.3183$.

4. Conclusions

In this paper we considered the late-time evolution of $f(R,T)$ gravity models, with the dark matter component of the theory being collisional. Due to the self-interaction of the dark matter component, the dark matter fluid had non-zero pressure, and thus can potentially affect the late-time evolution. In our study we investigated how this collisional component of dark matter can affect the late-time evolution. We considered two characteristic $f(R,T)$ gravity models, and by appropriately expressing the field equations as functions of the redshift parameter, we numerically solved the resulting field equations. As we demonstrated, the resulting picture corresponding to the collisional matter was qualitatively similar to that of non-collisional matter case, but there are differences in the deceleration to acceleration transition point, and also to the rate of the accelerating expansion. In all cases studied, however, it was found that a viable phenomenological evolution could be obtained by appropriately adjusting the free parameters of the theory. For the purposes of this study, we quantified our analysis by using the deceleration parameter and the total EoS parameter, and we demonstrated the effect of the collisional matter fluid by comparing the results with the ones corresponding to the ΛCDM model. Finally, we used an appropriate formalism for the late-time evolution, and we derived the field equations in an appropriate form for the late-time study. As we demonstrated, in this case too, a viable phenomenology can be achieved by $f(R,T)$ gravity in the presence of collisional matter. Notably, none of the collisional $f(R,T)$ gravity models crossed the phantom divide line, although the latter effect is supported by the observational data. It is worth further extending the formalism we employed in this paper to other theories, like Gauss–Bonnet theories of gravity, or perhaps $f(T)$ gravity, or even multidimensional gravity [66], and we hope to address some of these studies in a future work.

Author Contributions: Supervision, funding acquisition, conceptualization, software, investigation, M.Z.; methodology, software, formal analysis, writing review, M.Z.; writing original draft preparation, data curation, S.S.H.; Review and Editing, V.K.Oikonomou.

Funding: This research is supported by Higher Education Commission, Islamabad, Pakistan (Grant No. 5329/Federal/NRPU/R&D/HEC/2016).

Acknowledgments: Muhammad Zubair thanks the Higher Education Commission, Islamabad, Pakistan for its financial support under the NRPU project with grant number 5329/Federal/NRPU/R&D/HEC/2016.

Conflicts of Interest: The authors declare no conflict of interest.

References

1. Perlmutter, S.; Aldering, G.; Goldhaber, G.; Knop, R.A.; Nugent, P.; Castro, P.G.; Deustua, S.; Fabbro, S.; Goobar, A.; Groom, D.E.; et al. Measurements of Ω and Λ from 42 High-Redshift Supernovae. *Astrophys. J.* **1999**, *517*, 565–586. [CrossRef]
2. Riess, A.G.; Filippenko, A.V.; Challis, P.; Clocchiattia, A.; Diercks, A.; Garnavich, P.M.; Gilliland, R.L.; Hogan, C.J.; Jha, S.; Kirshner, R.P.; et al. Observational Evidence from Supernovae for an Accelerating Universe and a Cosmological Constant. *Astron. J.* **1998**, *116*, 1009–1038. [CrossRef]
3. Ade, P.A.R.; Aikin, R.W.; Barkats, D.; Benton, S.J.; Bischoff, C.A.; Bock, J.J.; Brevik, J.A.; Buder, I.; Bullock, E.; Dowell, C.D.; et al. Detection of B-Mode Polarization at Degree Angular Scales by BICEP2. *Phys. Rev. Lett.* **2014**, *112*, 241101. [CrossRef] [PubMed]
4. Nojiri, S.; Odintsov, S.D. Modified gravity with negative and positive powers of the curvature: Unification of the inflation and of the cosmic acceleration. *Phys. Rev. D* **2003**, *68*, 123512. [CrossRef]
5. Nojiri, S.; Odintsov, S.D.; Oikonomou, V.K. Modified Gravity Theories on a Nutshell: Inflation, Bounce and Late-time Evolution. *Phys. Rep.* **2017**, *692*, 1–104. [CrossRef]
6. Nojiri, S.; Odintsov, S.D. Unified cosmic history in modified gravity: From $F(R)$ theory to Lorentz non-invariant models. *Phys. Rep.* **2011**, *505*, 59–144. [CrossRef]
7. Weinberg, S. The cosmological constant problem. *Rev. Mod. Phys.* **1989**, *61*, 1. [CrossRef]
8. Ade, P.A.R.; Aghanim, N.; Armitage-Caplan, C.; Arnaud, M.; Ashdown, M.; Atrio-Barandela, F.; Aumont, J.; Baccigalupi, C.; Banday, A.J.; Barreiro, R.B.; et al. Planck 2013 results. XVI. Cosmological parameters. *Astron. Astrophys.* **2014**, *571*, A16.
9. Spergel, D.N.; Bean, R.; Dor, O.; Nolta, M.R.; Bennett, C.L.; Dunkley, J.; Hinshaw, G.; Jarosik, N.; Komatsu, E.; Page, L.; et al. Three-Year Wilkinson Microwave Anisotropy Probe (WMAP) Observations: Implications for Cosmology. *Astrophys. J. Suppl.* **2007**, *170*, 377. [CrossRef]
10. Eisenstein, D.J.; Zehavi, I.; Hogg, D.W.; Scoccimarro, R.; Blanton, M.R.; Nichol, R.C.; Scranton, R.; Seo, H.-J.; Tegmark, M.; Zheng, S.; et al. Detection of the Baryon Acoustic Peak in the Large-Scale Correlation Function of SDSS Luminous Red Galaxies. *Astrophys. J.* **2005**, *633*, 560–574. [CrossRef]
11. Capozziello, S.; Faraoni, V. *Beyond Einstein Gravity: A Survey of Gravitational Theories for Cosmology and Astrophysics*; Springer: Berlin, Germany, 2011.
12. Ferraro, R.; Fiorini, F. Modified teleparallel gravity: Inflation without an inflaton. *Phys. Rev. D* **2007**, *75*, 084031. [CrossRef]
13. Faraoni, V. *Cosmology in Scalar-Tensor Gravity*; Kluwer Academic Publishers: Alphen aan den Rijn, The Netherlands, 2004.
14. Sharif, M.; Zubair, M. Effects of Electromagnetic Field on the Dynamics of Bianchi type VI_0 Universe with Anisotropic Dark Energy. *Int. J. Mod. Phys. D* **2010**, *19*, 1957–1972. [CrossRef]
15. Sharif, M.; Zubair, M. Dynamics of a magnetized Bianchi VI_0 universe with anisotropic fluid. *Astrophys. Space Sci.* **2012**, *339*, 45. [CrossRef]
16. Sharif, M.; Zubair, M. Study of Bianchi I anisotropic model in $f(R,T)$ gravity. *Astrophys. Space Sci.* **2014**, *349*, 457. [CrossRef]
17. Brevik, I.; Gron, O.; de Haro, J.; Odintsov, S.D.; Saridakis, E.N. Viscous Cosmology for Early- and Late-Time Universe. *Int. J. Mod. Phys. D* **2017**, *26*, 1730024. [CrossRef]
18. Brevik, I.; Elizalde, E.; Odintsov, S.D.; Timoshkin, A.V. Inflationary universe in terms of a van der Waals viscous fluid. *Int. J. Geom. Meth. Mod. Phys.* **2017**, *14*, 1750185. [CrossRef]
19. Brevik, I.; Obukhov, V.V.; Timoshkin, A.V. Inflation in Terms of a Viscous van der Waals Coupled Fluid. *Int. J. Geom. Meth. Mod. Phys.* **2018**, *15*, 1850150. [CrossRef]
20. Buchdahl, H.A. Non-linear Lagrangians and cosmological theory. *Mon. Notice R. Astron. Soc.* **1970**, *150*, 1. [CrossRef]
21. Harko, T.; Lobo, F.S.N.; Nojiri, S.; Odintsov, S.D. $f(R,T)$ gravity. *Phys. Rev. D* **2011**, *84*, 024020. [CrossRef]

22. Azmat, H.; Zubair, M.; Noureen, I. Dynamics of shearing viscous fluids in $f(R,T)$ gravity. *Int. J. Mod. Phys. D* **2017**, *27*, 1750181. [CrossRef]
23. Baffou, E.H.; Salako, I.G.; Houndjo, M.J.S. Viscous Generalized Chaplygin Gas Interacting with $f(R,T)$ gravity. *Int. J. Geom. Meth. Mod. Phys.* **2017**, *14*, 1750051. [CrossRef]
24. Barrientos, E.; Lobo, F.S.N.; Mendoza, S.; Olmo, G.J.; Rubiera-Garcia, D. Metric-affine $f(R,T)$ theories of gravity and their applications. *Phys. Rev. D* **2018**, *97*, 104041. [CrossRef]
25. Pradhan, A.; Jaiswal, R. Magnetized string cosmological models of accelerated expansion of the Universe in $f(R,T)$ theory of gravity. *Int. J. Geom. Meth. Mod. Phys.* **2018**, *15*, 1850076. [CrossRef]
26. Zubair, M.; Azmat, H.; Noureen, I. Anisotropic stellar filaments evolving under expansion-free condition in $f(R,T)$ gravity. *Int. J. Mod. Phys. D* **2018**, *27*, 1850047. [CrossRef]
27. Shabani, H.; Ziaie, A.H. Bouncing cosmological solutions from $f(\mathsf{R},\mathsf{T})$ gravity. *Eur. Phys. J. C* **2018**, *78*, 397. [CrossRef]
28. Jamil, M.; Momenil, D.; Raza, M.; Myrzakulov, R. Reconstruction of some cosmological models in $f(R,T)$ cosmology. *Eur. Phys. J.* **2012**, *72*, 1999. [CrossRef]
29. Zubair, M.; Waheed, S.; Ahmad, Y. Static spherically symmetric wormholes in $f(R,T)$ gravity. *Eur. Phys. J. C* **2016**, *76*, 444. [CrossRef]
30. Zubair, M.; Mustafa, G.; Waheed, S.; Abbas, G. Existence of stable wormholes on a non-commutative-geometric background in modified gravity. *Eur. Phys. J. C* **2017**, *77*, 680. [CrossRef]
31. Moraes, P.H.R.S.; Sahoo, P.K. The simplest non-minimal matter-geometry coupling in the $f(R,T)$ cosmology. *Eur. Phys. J. C* **2017**, *77*, 480. [CrossRef]
32. Moraes, P.H.R.S.; Correa, R.A.C.; Lobato, R.V. Analytical general solutions for static wormholes in $f(R,T)$ gravity. *JCAP* **2017**, *7*, 29. [CrossRef]
33. Moraes, P.H.R.S.; Sahoo, P.K. Modelling wormholes in $f(R,T)$ gravity. *Phys. Rev. D* **2017**, *96*, 044038. [CrossRef]
34. Sharif, M.; Zubair, M. Thermodynamics in $f(R,T)$ theory of gravity. *JCAP* **2012**, *3*, 028. [CrossRef]
35. Sharif, M.; Zubair, M. Thermodynamics behavior of particular $f(R,T)$ gravity models. *J. Exp. Theor. Phys.* **2013**, *117*, 248. [CrossRef]
36. Sharif, M.; Siddiqa, A. Interaction of viscous modified Chaplygin gas with $f(R,T)$ gravity. *Mod. Phys. Lett. A* **2017**, *32*, 1750151. [CrossRef]
37. Myrzakulov, R. FRW Cosmology in $F(R,T)$ gravity. *Eur. Phys. J. C* **2012**, *72*, 2203. [CrossRef]
38. Odintsov, S.D.; Saez-Gomez, D. $f(R,T,R_{\mu\nu}T^{\mu\nu})$ gravity phenomenology and ΛCDM universe. *Phys. Lett. B* **2013**, *725*, 437. [CrossRef]
39. Haghani, Z.; Harko, T.; Lobo, F.S.N.; Sepangi, H.R.; Shahidi, S. Further matters in space-time geometry: $f(R,T,R_{\mu\nu}T^{\mu\nu})$ gravity. *Phys. Rev. D* **2013**, *88*, 044023. [CrossRef]
40. Sharif, M.; Zubair, M. Study of thermodynamics laws in $f(R,T,R_{\mu\nu}T^{\mu\nu})$ gravity. *JCAP* **2013**, *11*, 042. [CrossRef]
41. Sharif, M.; Zubair, M. Energy conditions in $f(R,T,R_{\mu\nu}T^{\mu\nu})$ gravity. *JHEP* **2013**, *12*, 079. [CrossRef]
42. Riess, A.G.; Strolger, L.-G.; Tonry, J.; Casertano, S.; Ferguson, H.C.; Mobasher, B.; Challis, P.; Filippenko, A.V.; Jha, S.; Li, W.; et al. Type Ia Supernova Discoveries at $z > 1$ from the Hubble Space Telescope: Evidence for Past Deceleration and Constraints on Dark Energy Evolution. *Astrophys. J.* **2004**, *607*, 665–687. [CrossRef]
43. Appleby, S.A.; Battye, R.A. Do consistent $F(R)$ models mimic General Relativity plus Λ? *Phys. Lett. B* **2007**, *654*, 7–12. [CrossRef]
44. Appleby, S.A.; Battye, R.A. Aspects of cosmological expansion in $F(R)$ gravity models. *J. Cosmol. Astropart. Phys.* **2008**. [CrossRef]
45. Sharif, M.; Zubair, M. Cosmological evolution of pilgrim dark energy. *Astrophys. Space Sci.* **2014**, *352*, 263. [CrossRef]
46. Sharif, M.; Zubair, M. Evolution of the universe in inverse and ln f(R) gravity. *Astrophys. Space Sci.* **2012**, *342*, 511–520. [CrossRef]
47. Mukherjee, A.; Banerjee, N. Acceleration of the Universe in $f(R)$ Gravity Models. *Astrophys. Space Sci.* **2014**, *352*, 893. [CrossRef]
48. Oikonomou, V.K.; Karagiannakis, N. Late-time cosmological evolution in $f(R)$ theories with ordinary and collisional matter. *Class. Quant. Grav.* **2015**, *32*, 085001. [CrossRef]

49. Oikonomou, V.K.; Karagiannakis, N.; Park, M. Dark energy and equation of state oscillations with collisional matter fluid in exponential modified gravity. *Phys. Rev. D* **2015**, *91*, 064029. [CrossRef]
50. Zubair, M. Phantom crossing with collisional matter in $f(T)$ gravity. *Int. J. Mod. Phys. D* **2016**, *25*, 1650057. [CrossRef]
51. Linder, E.V. Einsteins other gravity and the acceleration of the Universe. *Phys. Rev. D* **2010**, *81*, 127301. [CrossRef]
52. Wu, P.; Yu, H. Observational constraints on $f(T)$ theory. *Phys. Lett. B* **2010**, *693*, 415–420. [CrossRef]
53. Baffou, E.H.; Houndjo, M.J.S.; Rodrigues, M.E.; Kpadonou, A.V.; Tossa, J. Cosmological evolution in $f(R,T)$theory with collisional matter. *Phys. Rev. D* **2015**, *92*, 084043. [CrossRef]
54. Houndjo, M.J.S. Reconsrtruction of $f(R,T)$ gravity describing matter dominated and acelereated phases. *Int. J. Mod. Phys. D* **2012**, *21*, 1250003. [CrossRef]
55. Sharif, M.; Zubair, M.J. Cosmology of holographic and new Agegraphic $f(R,T)$ models. *Phys. Soc. Jpn.* **2013**, *82*, 064001. [CrossRef]
56. Sharif, M.; Zubair, M. Reconstruction and stability of $f(R,T)$ gravity with Ricci and modified Ricci dark energy. *Astrophys. Space Sci.* **2014**, *349*, 529–537. [CrossRef]
57. Jamil, M.; Momeni, D.; Raza, M.; Myrzakulov, R. Reconstruction of some cosmological models in $f(R,T)$ gravity. *Eur. Phys. J. C* **2012**, *72*, 1999. [CrossRef]
58. Sharif, M.; Zubair, M. Anisotropic Universe Models with Perfect Fluid and Scalar Field in $f(R,T)$ Gravity. *J. Phys. Soc. Jpn.* **2012**, *81*, 114005. [CrossRef]
59. Sharif, M.; Zubair, M. Energy Conditions Constraints and Stability of Power Law Solutions in $f(R,T)$ Gravity. *J. Phys. Soc. Jpn.* **2013**, *82*, 014002. [CrossRef]
60. Alvarenga, F.G.; Houndjo, M.J.S.; Monwanou, A.V.; Orou, J.B.C. Testing some $f(R,T)$ gravity models from energy conditions. *J. Mod. Phys.* **2013**, *4*, 130–139. [CrossRef]
61. Sharif, M.; Zubair, M. Cosmological reconstruction and stability in $f(R,T)$ gravity. *Gen. Relat. Grav.* **2014**, *46*, 1723. [CrossRef]
62. Jos Barrientos, O.; Guillermo, F. Comment on $f(R,T)$ gravity. *Phys. Rev. D* **2014**, *90*, 028501. [CrossRef]
63. Chang, J.; Adams, J.H.; Ahn, H.S.; Bashindzhagyan, G.L.; Christl, M.; Ganel, O.; Guzik, T.G.; Isbert, J.; Kim, K.C.; Kuznetsov, E.N.; et al. An excess of cosmic ray electrons at energies of 300–800 GeV. *Nature* **2008**, *456*, 362–365. [CrossRef] [PubMed]
64. Spergel, D.N.; Steinhardt, P.J. Observational Evidence for Self-Interacting Cold Dark Matter. *Phys. Rev. Lett.* **2000**, *84*, 3760. [CrossRef] [PubMed]
65. Kleidis, K.; Spyrou, N.K. A conventional approach to the dark-energy concept. *Astron. Astrophys.* **2011**, *529*, A26. [CrossRef]
66. Ernazarov, K.K. On non-exponential cosmological solutions with two factor spaces of dimensions m and 1 in the Einstein-Gauss-Bonnet model with a Λ-term. *Mod. Phys. Lett. A* **2017**, *32*, 1750202. [CrossRef]